Hindawi
Journal of Chemistry
Volume 2023, Article ID 7366941, 11 pages
https://doi.org/10.1155/2023/7366941

Research Article

Treatment of Industrial Saline Wastewater Using Eco-Friendly Adsorbents

Safiya Al Ajmi,[1] Murtuza Ali Syed,[1] Feroz Shaik,[2] Mohammed Nayeemuddin,[2] Deepanraj Balakrishnan,[2] and Venkata Ratnam Myneni[3]

[1]*National University of Science and Technology, Muscat, Oman*
[2]*Prince Mohammad Bin Fahd University, Al Khobar, Saudi Arabia*
[3]*Mettu University, Mettu, Ethiopia*

Correspondence should be addressed to Venkata Ratnam Myneni; venkata.rat@meu.edu.et

Received 7 August 2022; Revised 21 October 2022; Accepted 24 March 2023; Published 3 April 2023

Academic Editor: Vasant Madhav Wagh

Copyright © 2023 Safiya Al Ajmi et al. This is an open access article distributed under the Creative Commons Attribution License, which permits unrestricted use, distribution, and reproduction in any medium, provided the original work is properly cited.

The wastewater generated from the oil and gas sector is one of the major environmental issues. Varieties of techniques are employed for the treatment of generated wastewater. In this work, an attempt has been made to treat industrial saline wastewater from the oil and gas industry using a combination of synthesized biopolymer, chitosan, with graphene. Chitosan has been synthesized from a bioresource using marine spent. Chitosan was characterized using field emission scanning electron microscopy (FE-SEM), Fourier transform infrared (FT-IR) spectroscopy, energy dispersive X-ray (EDX) spectroscopy, and thermogravimetric analysis (TGA). Batch experiments were conducted by varying the composition of graphene viz 1, 2, 3, 4, and 5 w/w with respect to a fixed amount of chitosan. The percentage removal efficiency of chemical oxygen demand (COD), total dissolved solids (TDS), total suspended solids (TSS), turbidity, and oil and grease were evaluated. A combination of chitosan and graphene has effectively removed the pollutants present in oil produced water (OPW) compared to chitosan alone. The maximum percentage removal efficiencies of COD (84%), TDS (91%), TSS (80%), turbidity (95%), and oil and grease (99.9%) were obtained for a mixture of chitosan (0.5 g/100 mL) and 5 wt% graphenes. The Freundlich equilibrium isotherm model suited the adsorption data well.

1. Introduction

There is an alarming global concern for the scarcity of water, particularly in arid regions, and sustainable use of water, as mentioned in the United Nations 2030 sustainable development goals [1]. In this context, the management of industrial wastewater has gained profound importance among researchers. In the oil and gas industry, produced water is a term used to refer to wastewater, which is released as a by-product during the exploration of crude oil and gas. The oil produced water (OPW) generated during drilling and processing of oil and gas is one of the largest waste streams. It is salty water trapped in underground formations that can be brought to the surface during the oil and gas production. Treatment of OPW was required to meet disposal standards or to benefit end use. The composition of OPW differs from one well to another depending on the geographical conditions and the quality of the oil produced. OPW is typically saline with high total dissolved solids (TDS) and contains a lot of hazardous organic and inorganic compounds, dissolved gases, heavy metals, and naturally occurring radioactive materials. Most of the OPW was re-injected back to the oil wells to enhance oil production and part of it is considered for disposal to the environment [2–4].

Gravity separation [5], dissolved air flotation [5], membrane filtration [2], ion exchange, electrocoagulation [3], adsorption [6–8], advanced oxidation processes [9, 10], electrodialysis [11], chemical oxidation [12], biological aerated filters [13] and so on were some of the technologies used to treat the pollutants present in OPW. Enormous efforts have been made to develop cost-effective technologies for the treatment of OPW. Low-cost adsorbents prepared from kiwi peels have been used for the treatment of oil droplets from OPW. In the reference cited, the percentage

removal of oil droplets was linearly changed with adsorbent dosage, contact time, and pH [6]. In other work, activated carbon prepared from waste neem leaves and waste tea powder was employed to bleach the oil [7]. Black walnut media filters were used in a 48-in packed bed system for the removal of oil from OPW. A full breakthrough was achieved after 20–30 hours of operation [8]. Coagulants such as ferric chloride and aluminum sulphate have been utilized for the treatment of turbidity present in OPW. Aluminum sulphate was shown to be more efficient than ferric chloride in eliminating turbidity from OPW [3]. Chemical coagulation integrated with adsorption and heterogeneous photocatalysis was successfully employed to treat dissolved, dispersed oil droplets and organic matter present in OPW [10]. Nano titanium dioxide (TiO_2) embedded epoxy resin composites were tested in photocatalytic degradation of organics present in OPW, and an approximate 80% of reduction in organics was reported [14].

Derivatives of chitin and chitosan has been used to remove various pollutants from water due to high concentration of amino and hydroxyl functional groups, leading to significant adsorption of pollutants [15]. It is also becoming more popular due to properties including nontoxicity, natural abundance, biocompatibility, and biodegradability [16]. The removal of heavy metals and crude oil from synthetic and actual OPW was achieved using a chitosan-activated montmorillonite biocomposite. The biosorbent was able to remove 65 to 93% of heavy metals and 87% of the crude oil [17]. Chitosan, mixed with coagulants, was tested for the removal of oil from OPW. At pH 4 and 9, the oil removal efficiency of chitosan was reported to be 96 and 59%, respectively. The performance of chitosan was enhanced after adding different coagulants, carboxy methyl cellulose and aluminum sulphate at an average mixing time between 30 and 60 min [18]. The OPW treatment was investigated using microspheres made by reticulation of chitosan with sodium triphosphate (STP). The potential of these microspheres to remove oil from OPW was studied after they were packed in treatment columns. Microspheres having a porosity of around 80% were highly effective at removing oil, with removal rates above 90% [19].

Graphene oxide (GO), polybenzimidazole (PBI), and reduced GO (rGO) nanocomposite membranes were developed for the treatment of OPW from the oil and gas industry using the common blade coating and phase inversion method. Polydopamine (PDA), which has antifouling qualities, was used to cover the nanocomposite membranes. The oil removal efficiency of up to 99.9% was achieved by adding just a few percent GO to the PBI matrix [20]. The wastewater was treated using an environmentally friendly graphene oxide-chitosan (GC) composite hydrogel column (GCCHC). The GCCHC showed a good removal capability for cationic dyes, such as methylene blue and rhodamine B, as well as anionic dyes, such as methylene orange and congo red [21].

To the best of our knowledge, no research studies were reported in the literature for the treatment of OPW using the combined effect of chitosan with graphene. In this current study, an attempt has been made to investigate the effect of the combination of synthesized chitosan with graphene in suspension form for the treatment of OPW collected from an Oman oil field. The performance of the synthesized chitosan with graphene has been evaluated in terms of percentage removal efficiencies of total dissolved solids (TDS), total suspended solids (TSS), chemical oxygen demand (COD), turbidity, and oil and grease present in OPW.

Table 1: Initial composition of OPW.

Parameters	Values
COD (mg/L)	1147
TDS (mg/L)	6480
TSS (mg/L)	22
Turbidity (NTU)	55.1
Oil and grease (mg/L)	64.5
pH	9.02

2. Experimental

2.1. Materials and Methods. Waste shrimp shells were collected from the local fish market in Muscat, Sultanate of Oman. OPW was collected from the Oman oil field and stored at 4°C to avoid bacterial contamination. The initial composition of OPW is shown in Table 1. Graphene was obtained from an Indian research laboratory. Sodium hydroxide (NaOH) and hydrochloric acid (HCl) with 99.9% purity were procured from local markets. All reagents are of analytical grade and used as pure as supplied.

A Digital pH meter (JENWAY 3520) a water analysis kit (Eutech PCD 650) was used to measure the pH and TDS, respectively. A Turbidity meter (T-100 model, Singapore) was used to measure the turbidity. A COD digester (Hanna Instruments HI 839800 COD Digester, USA) with a photometer (Benchtop COD and a Multiparameter Photometer for Water Analysis-HI83099, USA) were used to measure the COD. Oil and grease were measured using a standard EPA 1664 method. A Digital weighing balance (Fabric Weight Balance Schroder-GSM200, Germany) was used to measure accurate weights of raw materials and chemicals. A JEOL JSM 7600F field emission scanning electron microscope (FE-SEM) was used to study the surface morphology of the prepared chitosan. Fourier transform infrared (FT-IR) spectroscopy spectra of the chitosan were recorded using a Perkin Elmer FT-IR spectroscopy between wave numbers 4000 to 400. A thermogravimetric analysis of the chitosan was carried out using SDT Q600, TA Instruments.

2.2. Preparation of Chitosan. Waste shrimp shells were washed thoroughly to remove the impurities on the surface of the shells. These were then dried under natural sunlight for 8 hours. The chitosan from dried waste shrimp shells was synthesized in three steps: demineralization, deproteinization, and deacetylation [22].

2.2.1. Demineralization. Dried shrimp shells were crushed to powder. A total of 40 g of shell powder was added to 10% hydrochloric acid in a ratio of 1 : 16 (weight/volume). This

mixture was kept for 24 hours at room temperature, making sure that the pH of the solution was maintained between 1 and 2.5. After 24 hours, the solution was filtered and then washed with distilled water until the pH of the solution became neutral. Finally, the sample was dried under the sun for 6 hours; the drying process was continued using the oven at 80°C until the entire moisture content was removed.

2.2.2. Deproteinization. Demineralized shell powder was added to 10% sodium hydroxide in a ratio of 1 : 16 (weight/volume). This mixture was kept for 48 hours at room temperature making sure that the pH of the solution was maintained between 11 and13. After 48 hours, the solution was filtered, and then the sample was washed with distilled water until the pH became neutral at value of 7.00. Finally, the water was removed, and the sample was decolorized with acetone.

2.2.3. Deacetylation. The product obtained from the deproteinization step is known as chitin. The chitin product was soaked in 60% sodium hydroxide for 48 hours at room temperature. Then the chitosan was obtained and washed with tap water until the pH became neutral. Finally, the synthesized chitosan after deacetylation was dried under the sun for 6 hours then the drying continued using the oven at 80°C to reduce the moisture content. The final chitosan was stored and used for subsequent characterization and adsorption experiments.

2.3. Characterization of Synthesized Chitosan. The prepared chitosan was characterized using FT-IR, FE-SEM, EDX, and TGA to study the structural surface morphology and decomposition characteristics. The spectra of synthesized chitosan obtained were compared with that of standard commercial chitosan.

2.4. Treatment of OPW with Synthesized Chitosan and Graphene. 0.5 g of prepared chitosan was added to 100 mL of OPW in a glass beaker and kept on a magnetic stirrer plate. The beaker was kept at room temperature with constant stirring at 500 RPM for 60 min. pH, turbidity, TDS, TSS, COD, and oil and grease were measured after one-hour treatment with the chitosan. Experiments were repeated by adding a calculated amount of graphene with chitosan in the adsorption process. The graphene concentration was varied from 1 to 5% (weight %) with respect to the amount of chitosan (0.5 g/100 mL) used in the experiments. All the parameters were measured after a contact time of 60 min. The percentage removal efficiency was estimated using the following equation [16]:

$$\text{Percentage removal efficiency} = \frac{\left(C_o - C_f\right)}{C_o} \times 100, \quad (1)$$

where c_0 and c_f are the initial and final concentrations in mg/L, respectively.

2.5. Adsorption Mechanism and Equilibrium Studies. The process of adsorption occurs when a fluid molecule (absorbate) is attached to the surface of a solid (adsorbent) and creates a molecular or atomic, as shown in Figure 1. This happens due to the existence of unbalanced or residual forces on the surface of a solid phase. The residual imbalance forces continue to attract and retain the molecular species as they reach the surface. The adsorbate is absorbed by the adsorbent in which the attraction between adsorbate and adsorbent arises due to the bonding forces, such as Van der Waals forces (weak forces) or covalent bond (strong forces). Adsorption can be divided into two forms: physical and chemical adsorption. Physical adsorption happens when the absorbent and adsorbate undergo weak Van der Waals forces, hydrogen bonding, polarity, and dipole-dipole interactions. Chemical adsorption is the process between the adsorbate and the surface of the adsorbent by chemical bonding or electron transfer. It is a permanent reaction known as activated adsorption. Physical adsorption is capable of forming a multilayer adsorption process that provides high adsorption capacity. On the contrary, chemical adsorption is limited to monolayer adsorption and selectively eliminates trace materials from aqueous solutions [23].

Adsorption isotherm models were used to represent the equilibrium relationship between the adsorbate adsorbed on the surface of biomass and the adsorbate present in the solution. Freundlich and Langmuir equilibrium models were represented by the following equations [16]:

$$\log q_e = \log K + \frac{1}{n}\log C_e, \quad (2)$$

$$\frac{1}{q_e} = \frac{1}{Q_{\max}} + \frac{C_e}{\left(b * Q_{\max}\right)}, \quad (3)$$

where "q_e" was the quantity of adsorbed metal ions (mg/g) and "C_e" was the equilibrium concentration (mg/L). K and n were the Freundlich equilibrium constants. $Q_{\max}$ represents the maximum adsorption and "b" was the affinity between the metal ions and the biomass.

3. Results and Discussion

3.1. Physical Characteristics of Synthesized Chitosan. The physical appearance of chitosan was white in color, odorless and in powder form. The physical characteristics indicated a good quality of chitosan similar to standard commercial chitosan was produced. Chitosan is deacetylated product of chitin with a degree of deacetylation that varies from 75% to 95%, and molecular weight between 50 and 200 kDa. Chitosan is composed of linear polycationic and heteropolysaccharide with β-1,4-2-deoxy-2-amino-D-glucopyranose and β-1,4-2-deoxy-2-acetamido-D-glucopyranose glycosidic linkages. The content of the amino group in chitosan varies in its physicochemical and biological properties. Chitosan is insoluble in water, basic pH solutions and organic solvents. However, it is soluble in weak acids and forms viscous solutions [24].

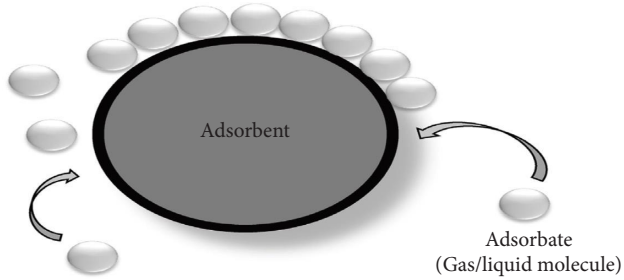

Figure 1: Adsorption process involving the adsorbent and adsorbate [23].

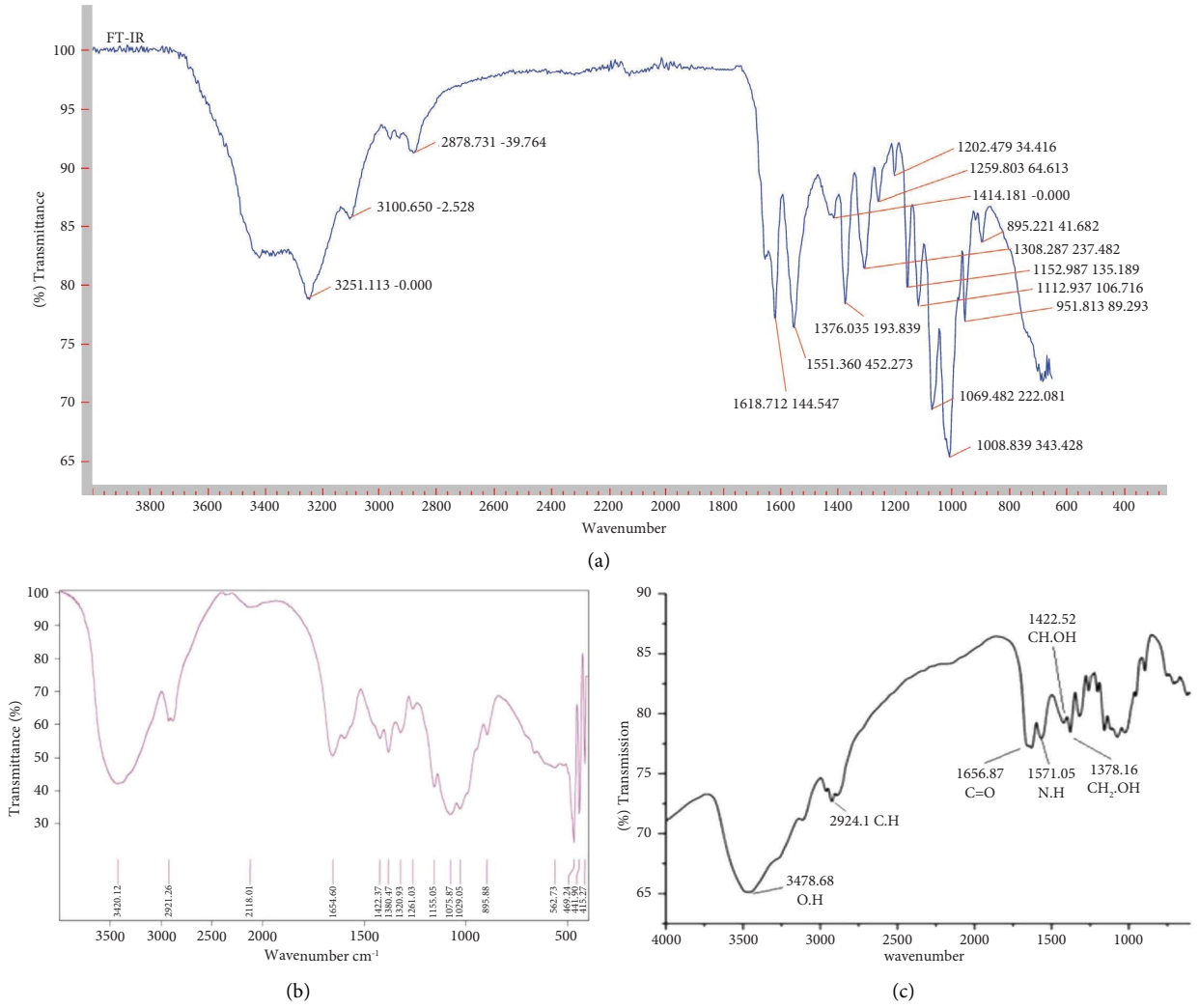

Figure 2: (a) FT-IR spectra of prepared chitosan. (b) FT-IR spectra of commercial chitosan [24]. (c) FT-IR spectra of synthesized chitosan [25].

3.2. FT-IR Analysis of Synthesized Chitosan. The FT-IR spectra of prepared chitosan indicated significant absorption bands to identify the characteristic functional groups, which were recorded at wave numbers between 4000 and 400 cm^{-1}. Figure 2(a) shows the infrared spectra of the prepared chitosan. The FT-IR spectra of the prepared chitosan were compared with the FT-IR spectra of standard commercial chitosan shown in Figure 2(b) [24] and that of prepared chitosan shown in Figure 2(c) [25]. The stretching vibrations of the –OH bond of the chitosan were observed at 3251 cm^{-1} (Figure 2(a)), which was similar to the –OH bond stretch in Figure 2(c) at 3478 cm^{-1}. An Alkyl C-H stretch group was observed at 3100 and 2878.7 cm^{-1} in the chitosan spectrum (Figure 2(a)) and the same stretch was indicated at 2928 cm^{-1} in Figure 2(b) and at 2924.1 cm^{-1} in Figure 2(c). An Alkenyl C=C stretch for chitosan was observed at 1618 cm^{-1} in Figure 2(a), and this coincides with that of 1654 cm^{-1} in Figure 2(b) and at 1656 cm^{-1} in Figure 2(c).

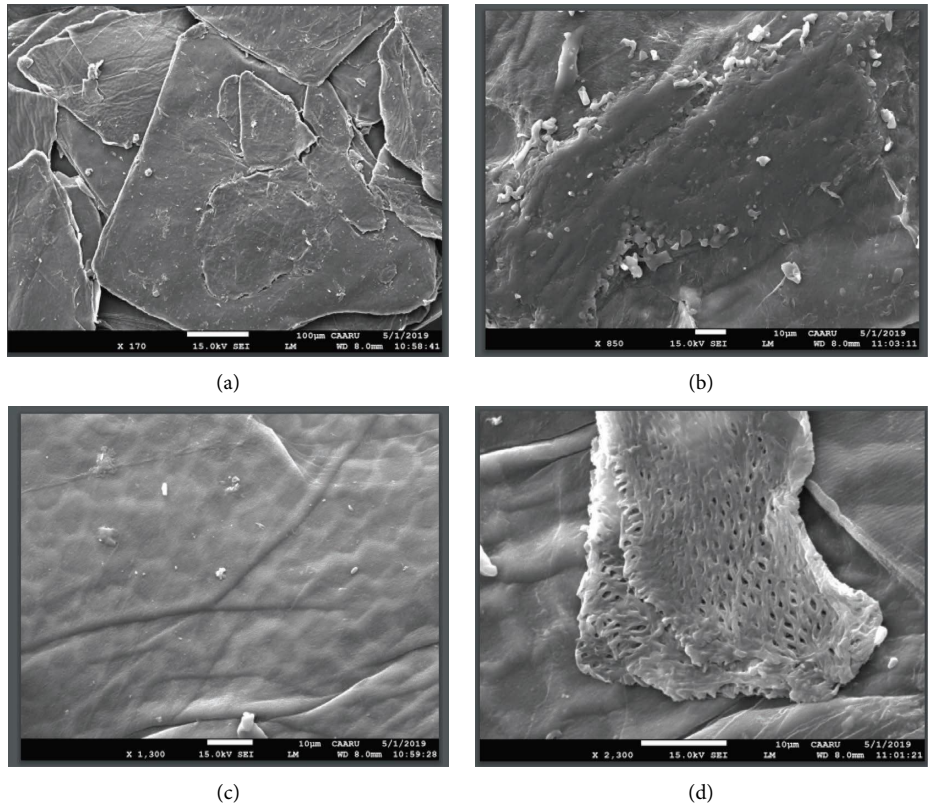

Figure 3: (a) SEM image of chitosan at ×170 (b) SEM image of chitosan at ×850 (c) SEM of chitosan image at ×1300 (d) SEM of chitosan image at ×2300.

The peaks at 1551 cm^{-1}, 1414 cm^{-1} and 1376 cm^{-1} shown in Figure 2(a) of chitosan were associated with the presence of the C=O stretching of the amide I band carbonyl group and the same was found at 1422 cm^{-1} and 1380 cm^{-1} in Figure 2(b) and at 1571 cm^{-1}, 1433 cm^{-1}, 1387 cm^{-1} in Figure 2(c). An Amine group peak was observed at 1308 cm^{-1} and an amino group ($-NH_2$) was 1069 to 1259 cm^{-1} for the chitosan in Figure 2(a). Finally, a pyranose ring was observed at 896 cm^{-1} for chitosan in Figure 2(a) and the same was observed at 895 cm^{-1} in Figure 2(b). From the FT-IR analysis, the synthesized chitosan had almost all functional groups found in a standard commercial chitosan.

3.3. FE-SEM Analysis of Synthesized Chitosan. The FE-SEM images for prepared chitosan are shown in Figures 3(a)–3(d) at different magnifications ×170, ×850, ×1300, ×2300 with an accelerating voltage of 15 KV, to explore the morphology and surface structure of the adsorbent. The image in Figure 3(a) exhibits lesser porosity with irregular texture and broken sections over the surface. The image in Figure 3(b) shows limited porosity and an irregular structure with pore sizes ranging from 8 mm to 10 μm. The image in Figure 3(c) exhibits a nonporous and smooth membranous phase and flat topography with pore sizes ranging from 8 mm to 1 μm. The image in Figure 3(d) shows a highly porous surface with various irregular segregated structures. Similar observations were reported by Hermiyatiet al. [26] and Kumari et al. [27].

3.4. SEM-EDX Analysis of Synthesized Chitosan. EDX analysis of the prepared chitosan was carried out and compared with a standard commercial chitosan spectrum. Figure 4(a) (Spectrum 3) and Figure 4(b) (Spectrum 2) were the spectra of prepared chitosan and Figure 4(c) is the spectra of standard commercial chitosan [28]. The prepared chitosan spectra exhibits peaks characteristic of aluminum (Al), silica (Si) and oxygen at 1.5 keV, 1.7 keV, and 0.5 keV, respectively, as shown in Figure 4(a). The spectra in Figure 4(b) indicated the existence of various elements, such as phosphorus (P) and calcium (Ca) at peaks 2 keV and 3.8 keV, which are related to carbonated hydroxyapatite. Carbon (C) showed the highest peak at 0.2 keV in Figure 4(b). The prepared chitosan spectra in Figures 4(a) and 4(b) were compared with a standard commercial chitosan spectra shown in Figure 4(c) and observed similar peaks for Al, Si, C, P, and O.

3.5. TGA Analysis. Thermogravimetric analysis/differential scanning calorimetry (TGA/DSC) was used to determine the decomposition temperature and to evaluate the thermal stability of the prepared chitosan. TGA-DSC analysis of prepared chitosan and standard commercial chitosan are shown in Figures 5(a) and 5(b), respectively. The TGA of prepared chitosan showed three steps of degradation: the first degradation occurs at 18.97°C with a weight loss of 0.02% due to the loss of initial moisture. The second stage of degradation occurred between 18.97 and 215.8 C with a loss

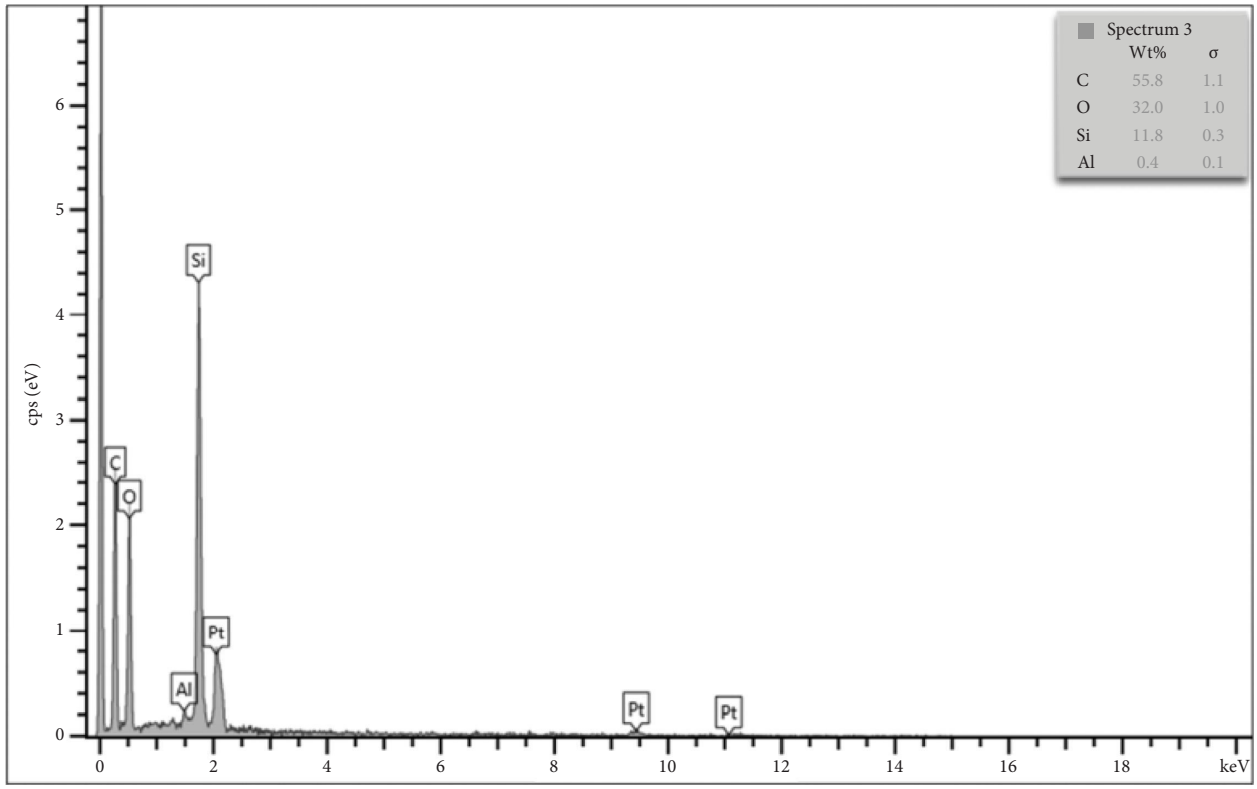

(a)

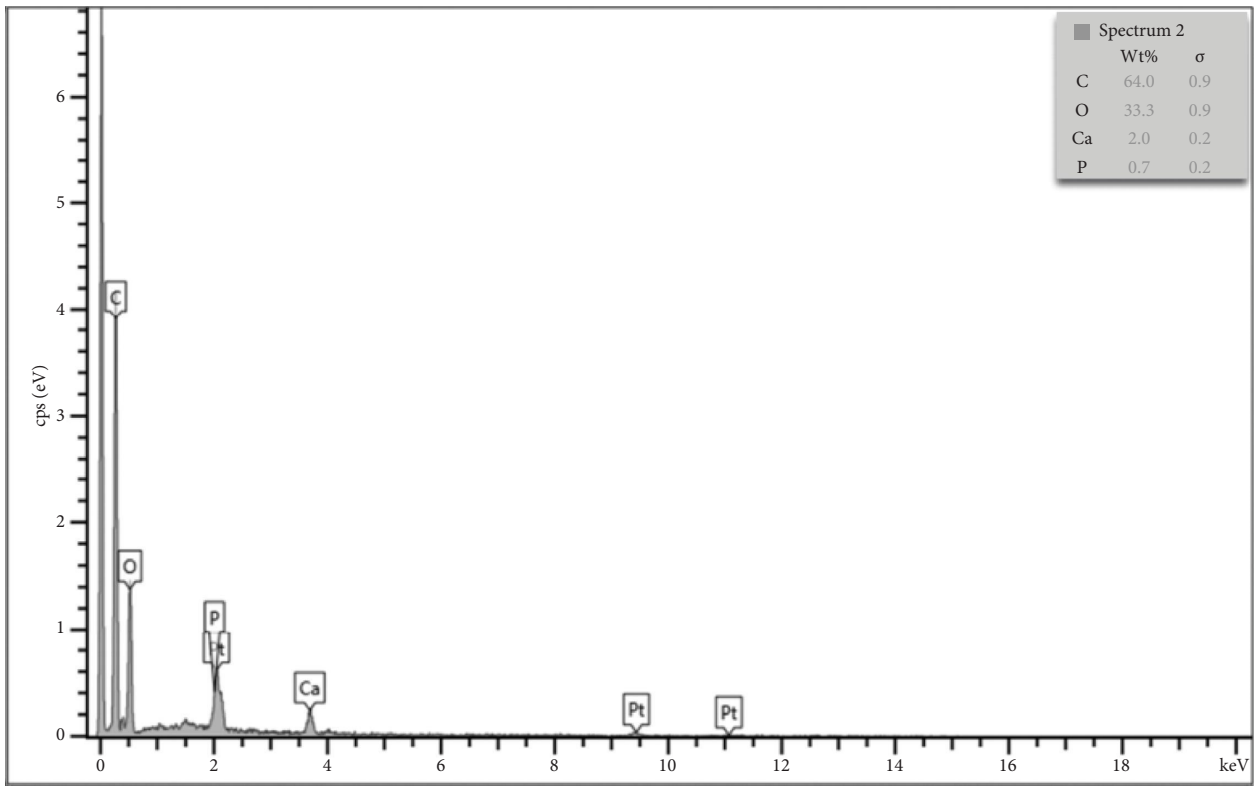

(b)

Figure 4: Continued.

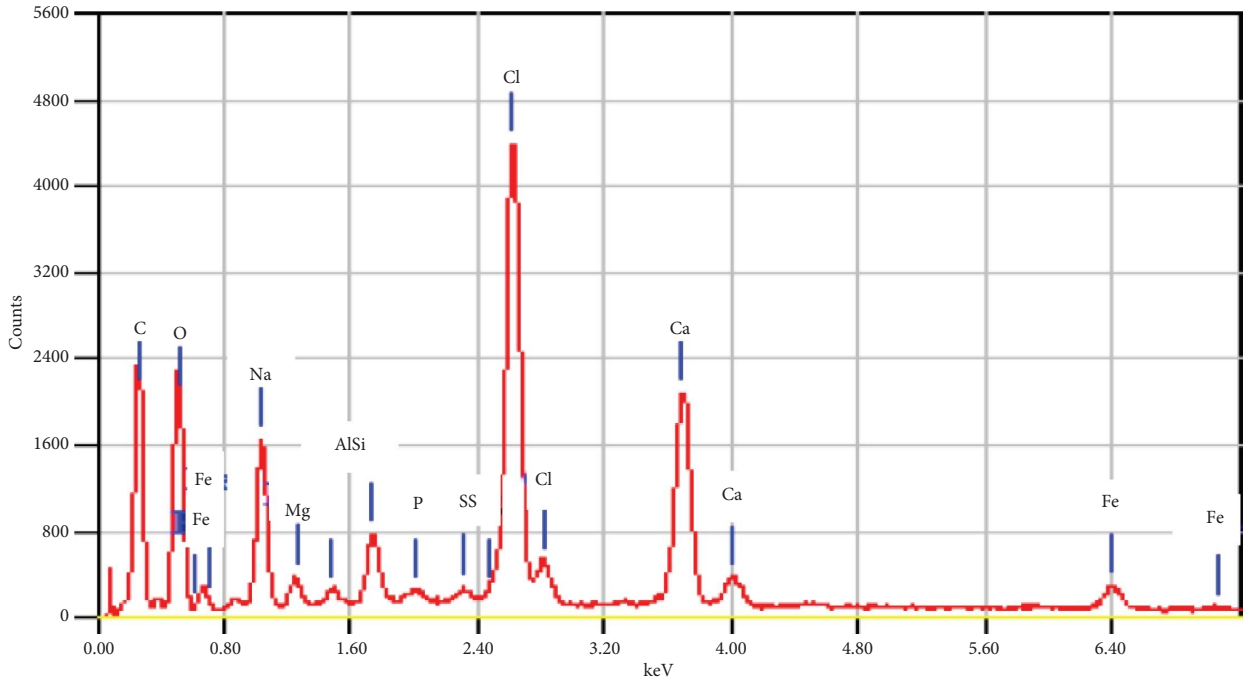

(c)

Figure 4: (a) EDX spectra of prepared chitosan. (b) EDX spectra of prepared chitosan. (c) EDX spectra of standard commercial chitosan [28].

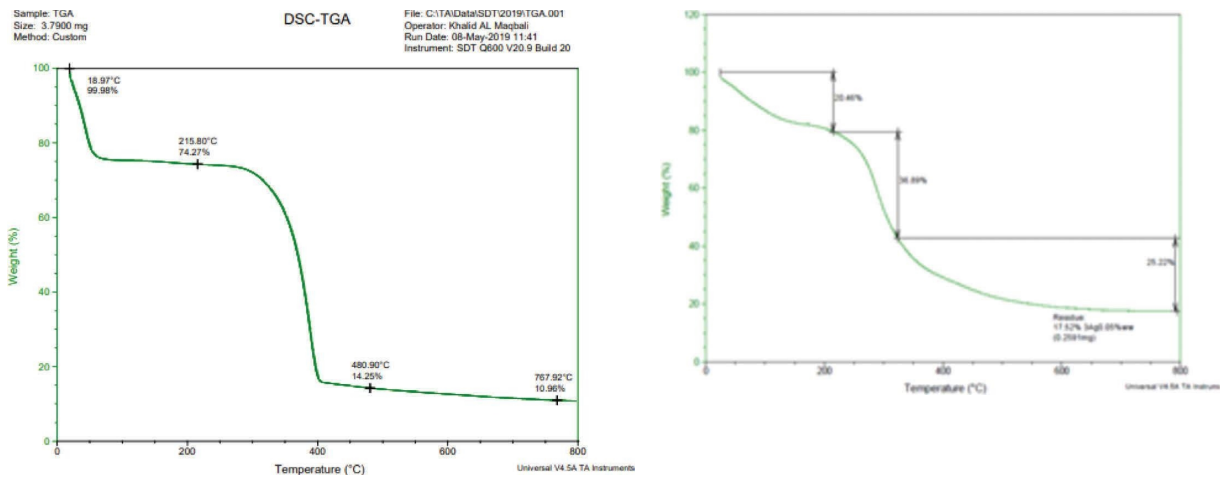

(a) (b)

Figure 5: (a) TGA of prepared chitosan. (b) TGA of standard chitosan [25].

of 25.63%, this may be due to the evaporation of solvents. The third step of degradation occurred between 215.8 and 480.9°C with 75.25% weight loss. The TGA of prepared chitosan degradation (Figure 5(a)) followed an almost similar trend to that of standard commercial chitosan degradation, as shown in Figure 5(b) [28].

3.6. OPW Treatment with Chitosan Alone. OPW was treated with prepared chitosan with and without the presence of graphene. The graphene concentration varied from 1 to 5% based on the weight of chitosan (0.5 g/100 mL). After 60 min of contact time, the relevant parameters were measured and the percentage removal efficiency was estimated. Figure 6 shows the percentage removal efficiency of parameters with chitosan alone. COD, TDS, TSS, turbidity, and oil and grease reduced to 38, 66, 5, 34, and 27%, respectively. The pH of OPW was redu ced from 9.02 to 7.67. At alkaline pH, the chitosan molecules are considered to be negatively charged and hence a repulsive force acts between the surface of chitosan and negatively charged ions present in OPW. The de-emulsification effect of oil and grease will be less in alkaline medium [19] and hence the percentage removal of oil

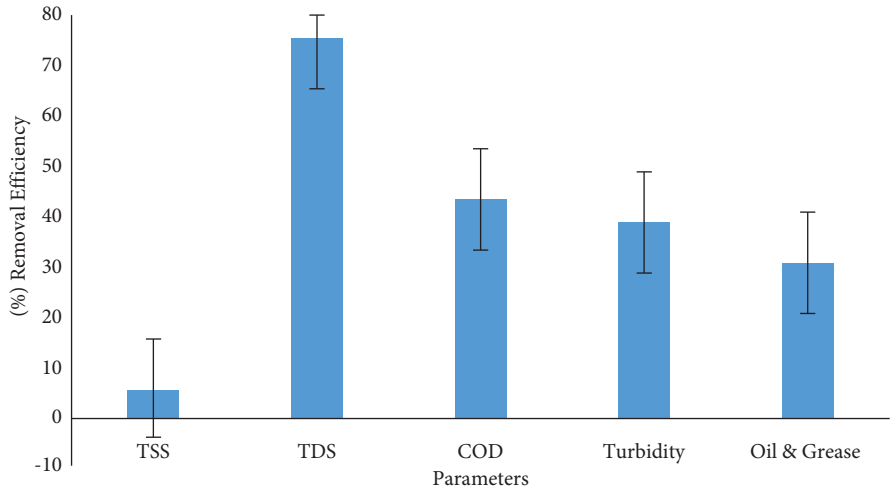

Figure 6: Percentage removal efficiency of parameters with chitosan.

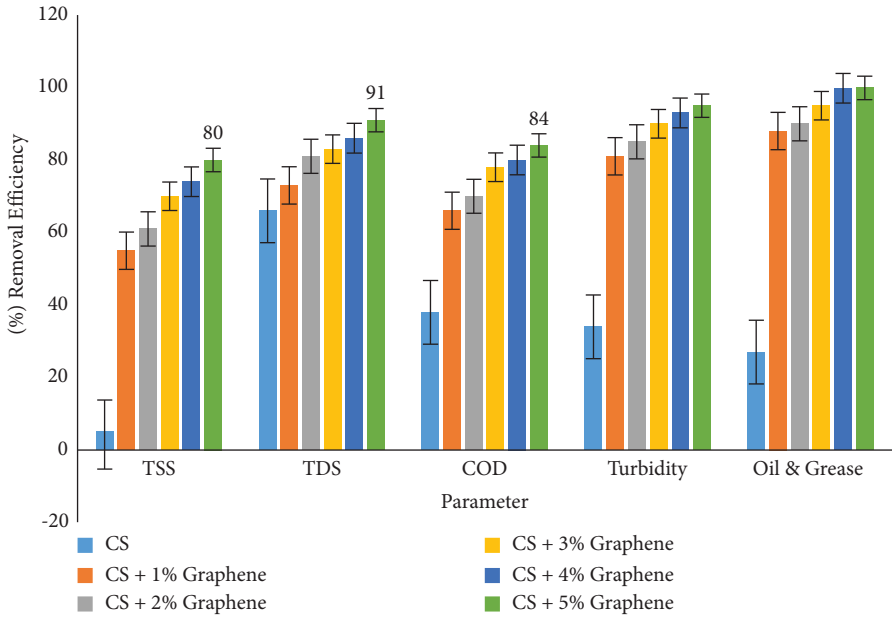

Figure 7: Comparison of percentage removal efficiencies with chitosan alone and in combination with graphene.

and grease was at a minimum compare to other parameters. The pH of the zero point of charge (pHzpc) of chitosan was reported to be 6.5. Protonation and deportation of chitosan amino groups depend on the pH of the OPW. The adsorption sites on the surface are protonated, and the sample surface is positively charged at pH values lower than pHzpc, while the sample surface is negatively charged at pH values higher than pHzpc. From the electrostatic interaction point of view, the positive charge of samples under acidic solution conditions should favor the adsorption of negatively charged species, and in basic solution, conditions may enhance the adsorption of positively charged species [29–31].

3.7. OPW Treatment with Combination of Chitosan and Graphene. Figure 7 shows the percentage removal efficiencies of parameters in OPW, when treated with chitosan (0.5 g) alone and in combination with various concentrations of graphene. As the concentration of graphene increases from 1 to 5% (0.005 g to 0.025 g), the percentage reduction of all parameters increases. The maximum removal efficiencies of parameters at 5% graphene are COD = 84%, TDS = 90.6%, TSS = 79.8%, turbidity = 94.8% and oil and grease = 99.9%. The pH of OPW redu ced from 9.02 to 5.77. Graphene has a large surface area (2630 m^2/g) and oleophilic in nature, and hence almost 100% of oil and grease was removed from OPW. The drop in pH also enhances the de-emulsification of oil droplets in an acidic medium and thereby increases the adsorption process. The other organic and inorganic pollutants present in OPW were also substantially reduced with the increase in graphene concentration along with chitosan. This may also be due to the availability of large active sites for the adsorption process. Table 2 presents a comparison of different adsorbents from the literature for oil removal with the present study.

Table 2: Comparison of oil removal in present study with the literature.

S.no	Adsorbent	Oil removal %	Reference
1	Modified kiwi peels	90	[6]
2	Bentonite	94.5	
3	Powdered activated carbon (PAC)	83.5	[32]
4	Deposited carbon (DC)	96.5	
5	Fish scales	93	[33]
6	Chitosan microspheres	90	[19]
7	Chitosan	99	[34]
8	Chitosan-5% graphene	99.9	Present work

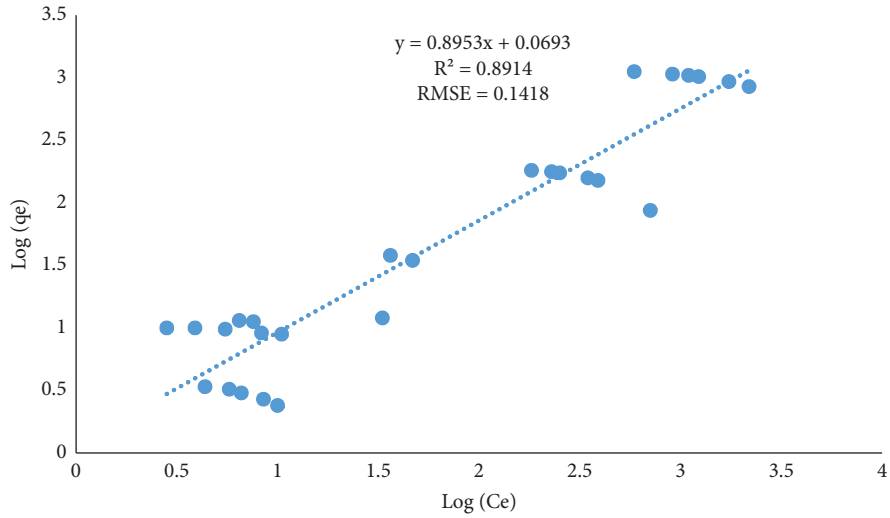

Figure 8: Freundlich isotherm.

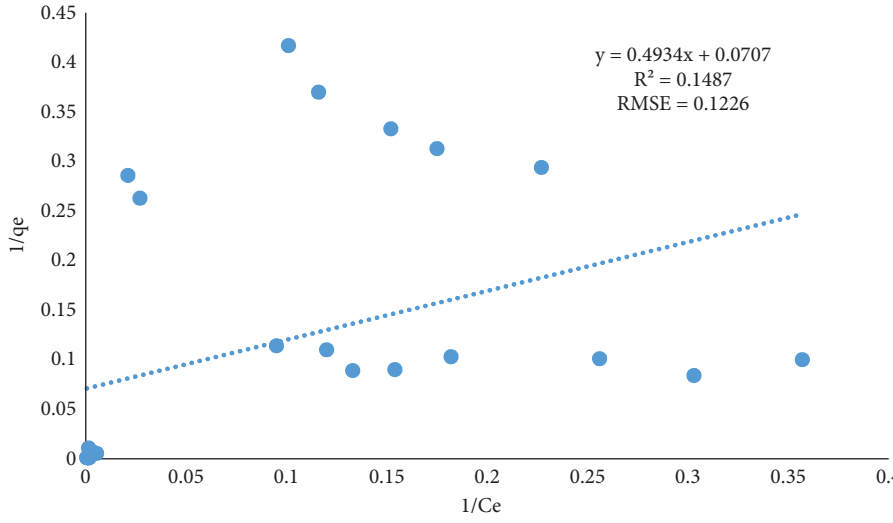

Figure 9: Langmuir isotherm.

The best performance of combined chitosan and graphene for the removal of pollutants from OPW (COD = 84%, TDS = 91%, and turbidity = 98.1%) is almost similar to the combined activated carbon, Iranian natural zeolite, and stabilized nano zero-valent iron for the removal of pollutants from grey water (COD = 85.75%, TDS = 91.81%, and turbidity = 98.1%) [35].

3.8. Adsorption Equilibrium Models. Freundlich and Langmuir isotherm models were applied to experimental data to find the best fit, as shown in Figures 8 and 9. Freundlich model seems to be a better fit for the adsorption of pollutants present in OPW on to adsorbents with a high correlation coefficient (R^2) and root mean square error (RMSE). This indicates that the adsorption mechanism is predominately

due to multilayer physical adsorption. In the Freundlich equilibrium model, the adsorption volume (K) was 1.173 mg/g, and the adsorption strength of adsorbents (n) was 1.117. In the Langmuir equilibrium model, the maximum adsorption capacity (Q_{max}) was 14.14 mg/g, and the affinity of pollutants (b) toward adsorbents was 0.143.

4. Conclusions

The treatment and reuse of OPW is one of the major issues in the oil and gas industry. Adsorption technology using low-cost adsorbents is widely employed for the removal of pollutants present in wastewater. The technology is considered to be efficient, cheap, and safe for the removal of pollutants present in wastewater streams. Adsorption has an excellent ability to remove pollutants at low concentrations with low energy consumption. Chitosan and graphene showed excellent adsorption characteristics in the removal of pollutants from wastewater streams. Chitosan has been synthesized from waste bioresource (waste shrimp shells collected from the fish market, Muscat area, and Sultanate of Oman). Chitosan has been characterized and compared with commercial standard chitosan. OPW was treated using prepared chitosan along with graphene. The performance of Chitosan in removing the pollutants present in OPW was enhanced in the presence of graphene. The maximum percentage removal efficiency of COD was = 84%, TDS was = 91%, TSS was = 80%, turbidity was = 95% and oil and grease was = 99.9%. These values were observed with chitosan (0.5 g/100 mL) and 5% (0.025 g) graphene. During the adsorption process, it was observed that the pH of OPW was redu ced from 9.02 to 5.77, which also enhanced the removal of pollutants present in OPW. The comparative studies showed that the combination of chitosan and graphene for the removal of pollutants from OPW performed more or less same with other adsorbents used for the treatment of pollutants from grey water.

Data Availability

All the data related to this work are available in the manuscript.

Conflicts of Interest

The authors declare that there are no conflicts of interest.

References

[1] United Nations, *SDG 6 Synthesis Report on Water and Sanitation*, UN-Water, New York, NY, USA, 2018.

[2] S. Nazirah, W. Ikhsan, N. Yusof, F. Aziz, and N. Misdan, "A review of oilfield wastewater treatment using membrane filtration over conventional technology," *Malaysian Journal of Analytical Sciences*, vol. 21, no. 3, pp. 643–658, 2017.

[3] A. Z. Rodriguez, H. Wang, L. Hu, Y. Zhang, and P. Xu, "Treatment of produced water in the Permian basin for hydraulic fracturing: comparison of different coagulation processes and innovative filter media," *Water*, vol. 12, no. 3, p. 770, 2020.

[4] K. Al Anezi, M. Belkharchouche, S. Alali, and W. Abuhaimed, "Oil produced water characterization in Kuwait and its impact on environment," *Desalination and Water Treatment*, vol. 56, no. 5, pp. 35–66, 2012.

[5] E. T. Igunnu and G. Z. Chen, "Produced water treatment technologies," *International Journal of Low Carbon Technologies*, vol. 9, no. 3, pp. 157–177, 2012.

[6] A. S. Jafer and A. A. Hassan, "Removal of oil content in oilfield produced water using chemically modified kiwi peels as efficient low-cost adsorbent," *Journal of Physics Conference Series*, vol. 1294, no. 7, Article ID 072013, 2019.

[7] F. Butt, M. Ali Syed, and F. Shaik, "Palm oil bleaching using activated carbon prepared from neem leaves and waste tea," *International Journal of Engineering Research and Technology*, vol. 13, no. 4, pp. 620–561, 2020.

[8] C. H. Rawlins and F. Sadeghi, "Experimental study on oil removal in nutshell filters for produced-water treatment," *SPE Production and Operations*, vol. 33, no. 1, pp. 145–153, 2018.

[9] M. J. Amiri, A. Faraji, M. Azizi, B. G. Nejad, and M. Arshadi, "Recycling bone waste and cobalt-wastewater into a highly stable and efficient activator of peroxymonosulphate for dye and HEPES degradation," *Process Safety and Environmental Protection*, vol. 147, pp. 626–641, 2021.

[10] P. C. Silva, N. P. Ferraz, E. A. Perpetuo, and Y. J. O. Asencios, "Oil produced water treatment using advanced oxidative processes: heterogeneous-photocatalysis and photo-Fenton," *Journal of Sedimentary Environments*, vol. 4, no. 1, pp. 99–107, 2019.

[11] P. Sosa-Fernandez, J. W. Post, H. Bruning, F. A. M. Leermakers, and H. H. M. Rijnaarts, "Electrodialysis-based desalination and reuse of sea and brackish polymer flooding produced water," *Desalination*, vol. 447, pp. 120–132, 2018.

[12] S. Shokrollahzadeh, F. Golmohammad, N. Naseri, H. Shokouhi, and M. Arman-mehr, "Chemical oxidation for removal of hydrocarbons from gas–field produced water," *Procedia Engineering*, vol. 42, pp. 942–947, 2012.

[13] D. Su, J. Wang, K. Liu, and D. Zhou, "Kinetic performance of oil-field produced water treatment by biological aerated filter," *Chinese Journal of Chemical Engineering*, vol. 15, no. 4, pp. 591–594, 2007.

[14] S. Murtuza Ali, M. Amit Kumar, and S. Feroz, "Investigation of epoxy resin/nano-TiO_2 composites in photocatalytic degradation of organics present in oil-produced water," *International Journal of Environmental Analytical Chemistry*, vol. 100, pp. 1–18, 2020.

[15] A. Bhatnagar and M. Sillanpää, "Applications of chitin- and chitosan-derivatives for the detoxification of water and wastewater--a short review," *Advances in Colloid and Interface Science*, vol. 152, no. 1-2, pp. 26–38, 2009.

[16] M. J. Amiri, M. Bahrami, M. Badkouby, and I. K. Kalavrouziotis, "Greywater treatment using single and combined adsorbents for landscape irrigation," *Environmental Processes*, vol. 6, no. 1, pp. 43–63, 2019.

[17] R. Akhbarizadeh, F. Moore, D. Mowla, and B. Keshavarzi, "Improved waste-sourced biocomposite for simultaneous removal of crude oil and heavy metals from synthetic and real oilfield-produced water," *Environmental Science and Pollution Research*, vol. 25, no. 31, pp. 31407–31420, 2018.

[18] R. Hosny, M. Fathy, M. Ramzi, T. Abdel Moghny, S. E. M. Desouky, and S. A. Shama, "Treatment of the oily produced water (OPW) using coagulant mixtures," *Egyptian Journal of Petroleum*, vol. 25, no. 3, pp. 391–396, 2016.

[19] I. C. D. S. Grem, B. N. B. Lima, W. F. Carneiro, Y. G. D. C. Queirós, and C. R. E. Mansur, "Chitosan microspheres applied for removal of oil from produced water in the oil industry," *Polimeros*, vol. 23, no. 6, pp. 705–711, 2013.

[20] A. A. Alammar, S. H. Park, C. J. Williams, B. Derby, and G. Szekely, "Oil-in-water separation with graphene-based nanocomposite membranes for produced water treatment," *Journal of Membrane Science*, vol. 603, pp. 118007–118011, 2020.

[21] T. S. Vo, T. T. B. C. Vo, J. W. Suk, and K. Kim, "Recycling performance of graphene oxide-chitosan hybrid hydrogels for removal of cationic and anionic dyes," *Nano Convergence*, vol. 7, no. 1, p. 4, 2020.

[22] F. Nessa, S. M. Masum, M. Asaduzzaman, S. K. Roy, M. M. Hossain, and M. S. Jahan, "A Process for the preparation of chitin and chitosan from prawn shell waste," *Bangladesh Journal of Scientific and Industrial Research*, vol. 45, no. 4, pp. 323–330, 1970.

[23] N. N. Rudi, M. S. Muhamad, L. Te Chuan et al., "Hasnida Harun: evolution of adsorption process for manganese removal in water via agricultural waste adsorbents," *Heliyon*, vol. 6, no. 9, Article ID 05049, 2020.

[24] T. K. Varun, S. Senani, N. Jayapal et al., "Extraction of chitosan and its oligomers from shrimp shell waste, their characterization and antimicrobial effect," *Veterinary World*, vol. 10, no. 2, pp. 170–175, 2017.

[25] S. Yasmeen, M. K. Kabiraz, B. Saha, M. R. Qadir, M. A. Gafur, and S. M. Masum, "Chromium (VI) ions removal from tannery effluent using chitosan-microcrystalline cellulose composite as adsorbent," *IRJPAC*, vol. 10, no. 4, pp. 1–14, 2016.

[26] I. Hermiyati, I. Iswahyuni, and S. Juhana, "Synthesis of chitosan from the scales of starry trigger fish (Abalistes-Stelaris)," *Oriental Journal of Chemistry*, vol. 35, no. 1, pp. 377–383, 2019.

[27] S. Kumari, P. Rath, and S. H. Kumar, "Chitosan from shrimp shell (*Crangon crangon*) and fish scales (*Labeorohita*): extraction and characterization," *African Journal of Biotechnology*, vol. 15, no. 24, pp. 1258–1268, 2016.

[28] H. E. Ghannam, A. S. Talab, N. V. Dolgano, A. M. S. Husse, and N. M. Abdelmagui, "Characterization of chitosan extracted from different crustacean shell wastes," *Journal of Applied Sciences*, vol. 16, no. 10, pp. 454–461, 2016.

[29] M. Ziegler-Borowska, D. Chelminiak, H. Kaczmarek, and A. Kaczmarek-Kędziera, "Effect of side substituents on thermal stability of the modified chitosan and its nanocomposites with magnetite," *Journal of Thermal Analysis and Calorimetry*, vol. 124, no. 3, pp. 1267–1280, 2016.

[30] M. A. Torres, M. M. Beppu, and C. C. Santana, "Characterization of chemically modified chitosan microspheres as adsorbents using standard proteins (Bovine serum albumin and lysozyme)," *Brazilian Journal of Chemical Engineering*, vol. 24, no. 3, pp. 325–336, 2007.

[31] S. Nallakukkala, B. Lal, and F. Shaik, "Kinetic and isothermal investigations in elimination of iron metal from aqueous mixture by using natural adsorbent," *International journal of Environmental Science and Technology*, vol. 18, no. 7, 2020.

[32] K. Okiel, M. El-Sayed, and M. Y. El-Kady, "Treatment of oil–water emulsions by adsorption onto activated carbon, bentonite and deposited carbon," *Egyptian Journal of Petroleum*, vol. 20, no. 2, pp. 9–15, 2011.

[33] T. Lutfee, J. A. Al-Najar, and F. M. Abdulla, "Removal of oil from produced water using biosorbent," *IOP Conference Series: Materials Science and Engineering*, vol. 737, no. 1, Article ID 012198, 2020.

[34] A. L. Ahmad, S. Sumathi, and B. H. Hameed, "Chitosan: a natural biopolymer for the adsorption of residue oil from oily wastewater," *Adsorption Science and Technology*, vol. 22, no. 1, pp. 75–88, 2004.

[35] M. J. Amiri, M. Bahrami, M. Badkouby, and I. K. Kalavrouziotis, "Greywater treatment using single and combined adsorbents for landscape irrigation," *Environmental Processes*, vol. 6, no. 1, pp. 43–63, 2019.